Carbon Vol. 23, No. 5, pp. 501–511, 1985
Printed in the U.S.A.

0008-6223/85 $3.00 + .00

DOPED CARBON BLACK CATALYST SUPPORTS: II. MAGNETIC, MÖSSBAUER, AND CATALYTIC STUDIES OF IRON/CARBON SYSTEMS

L. N. MULAY,† A. V. PRASAD RAO, P. L. WALKER, JR. and K. J. YOON
Department of Materials Science and Engineering, The Pennsylvania State University, University Park, PA 16802, U.S.A.

and

M. A. VANNICE
Department of Chemical Engineering, The Pennsylvania State University, University Park, PA 16802, U.S.A.

(*Received* 27 *August* 1984; *in revised form* 13 *November* 1984)

Abstract—In continuation of our earlier investigation of carbon-supported Fe catalysts, a systematic study of diamagnetic susceptibility and ESR spectroscopy was carried out on "as-received", graphitized, and boron-doped carbon blacks. This characterization showed the Fermi level (E_f) of the graphitic carbon decreased with boron doping. These carbon supports were used for dispersing small Fe crystallites, which were further characterized by appropriate *in situ* magnetization measurements and Mössbauer Spectroscopy. Observations showed that all Fe/C catalysts were superparamagnetic yielding particle diameters in the range of 3.5–5.5 nm. From the reaction rates obtained for CO hydrogenation over these catalysts, activation energies, product distributions, and turnover frequencies were computed. These results were compared with Fe/Al_2O_3 and Fe/SiO_2 catalysts. The iron dispersed on boronated carbons showed a small increase in turnover frequency for CO hydrogenation as compared with Fe dispersed on undoped carbons. A seven-fold change in the E_f level of the carbon supports produced only a twofold change in activity, and consequently a strong interaction between the iron and carbon could not be confirmed.

Key Words—Carbon black, catalyst, magnetic susceptibility, Mössbauer spectroscopy, iron.

1. INTRODUCTION

In a previous publication[1] we reported the characterization of boron-doped and undoped carbon blacks by magnetic susceptibility measurements at selected temperatures in the range 80–300 K, and by ESR spectroscopy at cryogenic temperatures (~100 K) and room temperature (300 K). Some of the graphitized carbons were boronated up to 260 ppm at heat treatment temperatures of either 2073 or 2773 K, and they showed that the diamagnetic susceptibility decreased significantly when the boronation was done at the higher temperature of 2773 K. Here it was clearly established that the magnitude of the diamagnetic susceptibility per gram (χ) decreased systematically with boron doping. From these results appropriate conduction band parameters were calculated and a decrease in the Fermi level (E_F) of the carbons was found as the boron doping level increased.

In this paper we present the characterization of Fe dispersed on various carbons by magnetization measurements, studied as a function of the applied field and temperature, which yielded information on the Fe particle size. Furthermore, selected Fe/carbons were characterized by ^{57}Fe Mössbauer spectroscopy, which supplemented the results obtained from the magnetization measurements. The kinetic parameters of these catalysts in CO hydrogenation were measured, and correlations were sought between catalytic behavior and the state of the catalysts. The rationale for changing the electronic nature of the substrate by boron doping was explained in Part I of this paper[1].

2. EXPERIMENTAL

A description of the various carbon blacks supplied by the Cabot Corporation, the boronation procedures, and analysis of the boron content has been given previously[1]. The carbon-supported iron catalysts listed in Table 1 were prepared by an incipient wetness technique using approximately 1 cc/g of an amount of iron nitrate (Fisher Scientific), dissolved in distilled and deionized water to give the required metal loadings[2]. The solution was added dropwise to the dried and weighed support at room temperature using a dropper, with vigorous stirring between successive additions. The impregnated catalysts were then oven-dried in air for 16 hr at 393 K, bottled and stored in a desiccator for later use. Iron weight loadings of the fresh unreduced catalysts were determined by neutron activation analysis at the Breazeale Nuclear reactor at PSU. Iron dispersions (fractions exposed) and crystallite sizes from chemisorption measurements were determined by irreversible CO adsorption at 195K in a fashion described previously[3].

The magnetization (σ, emu/g) measurements were carried out using a sensitive Faraday microbalance described by Mulay[4]. Measurements were first carried out on the fresh samples containing Fe^{3+} ions as a function of the

†Address enquiries to this author at 136 Materials Research Laboratory, or to M. A. Vannice, Chem. Eng. Dept.

Table 1. Properties of supported iron catalysts

Catalyst	Support	B-Level (ppm)	N_2 BET Surface Area ($m^2 \cdot g\text{-support}^{-1}$)
4.8% Fe/MC	Monarch 700	nil	206
4.8% Fe/GMC	GMC	nil	82*
5.3% Fe/BGMC1	BGMC1	170	92*
5.2% Fe/BGMC2	BGMC2	260	87*
4.9% Fe/BGMC4	BGMC4	140	-
4.9% Fe/BGMC5	BGMC5	220	110
4.3% Fe/C-2	Carbolac-2	nil	850
5.0% Fe/CSX	CSX 203	nil	1400
5.8% Fe/SiO_2	Cabosil SiO_2	nil	160
10% Fe/Al_2O_3	n-Al_2O_3	nil	245

*Using $CO_{(ad)}/Fe_s = 0.5$ (ref. 2)

applied field, H, and the measurement temperature, T_m. The entire balance was evacuated and the samples were then reduced *in situ* by flowing 99.999% H_2 (Matheson Co.) at 673 K for 16 hr by using an appropriate furnace surrounding the sample chamber of the balance[2]. The same ultrapure H_2 was used for *in situ* Mössbauer experiments which are described at the end of this section. After cooling the sample to room temperature, magnetization measurements were carried out at various temperatures and at fields up to 10 kOe.

Mössbauer spectra of ^{57}Fe were obtained with a Mössbauer drive unit and a transducer operating in a constant acceleration mode (Austin Associates), using a 50 mCi ^{57}Co source in an Rh matrix (New England-Nuclear Company), which gave an intrinsic narrow line for the source. The 14.4 keV γ-rays were used and detected by a proportional counter containing 90% Ar and 10% methane (Reuter-Stokes Co.). A He–Ne laser interferometer was used for absolute calibration. The other electronic units consisted of a multi-channel analyzer (Nuclear Data 100) with 1024 channels, a preamplifier, high-voltage supply, and an analog-to-digital converter (Nuclear Data 570). The *in situ* Mössbauer spectra were obtained using a specially designed cell similar to that described by Delgass and coworkers[5]. All results are reported with respect to an NBS-Fe foil. The gases used, H_2 (99.999% pure) and He (99.999% pure) were obtained from the Matheson Co. These were further purified by passing through an Oxytrap and a molecular sieve (Alltech Associates). The flow rates were controlled by mass flow controllers (Brooks Division).

The microreactor flow system used for studying CO hydrogenation was the same as that used by Jung[2]. It consisted of a fixed bed reactor held in a fluidized sand bath in which the temperature could be varied from 300 to 773 K within ±0.1 K. A standard pretreatment was used for a set of reactor runs to compare the behavior of the various catalysts, including Fe/Al_2O_3 and Fe/SiO_2. The samples were heated in flowing H_2 (50 cm/min) at a constant temperature of 393 K for 30 min before continuing to heat to 723 K. The fresh catalyst was held at 723 K for 16 hr to ensure complete reduction to Fe before cooling under flowing H_2 to a selected reaction temperature in the range of 488–548 K. The reactor system was operated at a total pressure of one atmosphere. The individual reactant gas flows were monitored by calibrated mass flowmeters (Model A11-100, Hastings–Raydist), which were accurate to ±0.1 cc/min. The catalyst charge in the reactor was small, usually less than 0.5 g. The analysis of the exit gas was conducted using a gas chromatograph (Perkin–Elmer, Sigma 3) with subambient temperature programming, Chromosorb 102 columns. Peak areas were determined by a Sigma 1 electronic integrator (Perkin–Elmer).

In addition to the ultrapure H_2 and He, CO (99.999% pure from the Matheson Co.) was used. The H_2 was passed through a Deoxo unit (Engelhard Industries, Inc.), a 5A molecular sieve trap, and finally through an Oxytrap (Alltech Associates) before being used for catalytic studies. The CO was passed through a heated 5A molecular sieve trap to remove any water and carbonyls. The He was passed through a Drierite molecular sieve gas purifier (Alltech Associates) and an Oxytrap.

To achieve steady-state operation in the reactor, the reactant gases were normally passed over the catalyst for 20 min prior to sampling the exit stream for analysis. After sampling, the CO flow was stopped, and H_2 alone was flowed for 20 min to help regenerate and maintain a clean metal surface for the subsequent reaction period. This bracketing technique has been found to be very effective in eliminating possible complications arising from catalyst deactivation[2].

High space velocities of 1000–3000 hr^{-1} were typically used to keep CO conversions around 5% or less. This provided conversion data from a differential reactor, thereby minimizing heat and mass transfer effects, eliminating any significant effects due to product inhibition, and giving initial rates with minimum complication from secondary reactions. Rates of both methane formation and CO conversion to any and all hydrocarbon products

were based on accurate CO flow rates, coupled with carbon mass balances on the product stream, which were determined directly from gc analysis.

3. RESULTS AND DISCUSSION

3.1 *Magnetization measurements*

This section is concerned especially with the superparamagnetic particles of Fe, etc. species on carbon. Hence, we shall succinctly outline important principles of superparamagnetism, which have a direct bearing on our research. Ferromagnetic metals, such as Fe, Co, Ni, and ferrimagnetic insulators such as γ-Fe_2O_3 and Fe_3O_4, show the well-known hysteresis curve, which stems from their multi-domain structure. In their unmagnetized state, the unpaired electrons (spins) associated with each atom (or structural unit) have a net spontaneous magnetic "moment (μ_s)" or magnetization (σ_s). Between the domains, a "Bloch wall" is formed, with spins curled up in a helical fashion. When an external field (H) is applied, the magnetic moments align "parallel" to the applied field, even at modest values ~3000 Oe (Oersteds) at room temperature, which happens to be below the Curie temperature (T_c). This T_c is a critical temperature above which the magnetization (σ_s) disappears and follows a paramagnetic behavior. Each domain consists of myriads of spins. One can imagine small particles within each domain having different volumes (V_1, V_2, . . . V_i). These *subdomain* particles, which consist of several thousand spins, are known as S.P. (superparamagnetic) clusters and have large magnetic moments of several thousand B.M. (Bohr Magnetons; one BM = $eh/4\pi mc$, where the symbols have their usual meaning[4, 6, 7]. When such S.P. particles are well-dispersed on a substrate (e.g. SiO_2, Al_2O_3, carbon, etc.), there is no magnetic interaction between their net moments. Hence, the ideal S.P. particles behave in the same manner as "magnetically dilute" paramagnetic ions, such as Fe^{3+} ($^6S_{5/2}$ ion, with 5 *d* spins, which show an *effective* B.M. number (μ_{eff}) of $\sqrt{5(5+2)} = 5.96$). Such ions can orient parallel and antiparallel to H, according to the Boltzmann statistics, independently of each other, and experience thermal fluctuations. For paramagnetic ions, the susceptibility ($\chi = \sigma/H$) and the μ_{eff} are good parameters for interpretation of magnetic results. However, for the S.P. particles with a giant B.M. number of ~10^4, the per gram magnetization (σ) is a good parameter. The σ increases with increasing H, and with decreasing temperature (T). Therefore, it is customary to measure σ at constant H and varying T, and vice-versa. When the relative magnetization σ/σ_s (where σ_s is the saturation magnetization) is plotted as a function of H/T, one obtains an excellent superposition of data points, and there is no coercive force ($H_c = 0$); that is, there is no hysteresis, as in the well-known bulk ferromagnetic or ferrimagnetic materials[4, 7]. Therefore, one can apply the classical Langevin function, first derived from the non-interacting paramagnetic spins, to the non-interacting (ideal) S.P. particles. Thus,

$$\sigma/\sigma_s = \mathrm{Coth}\,(\mu_c H/kT) - (kT/\mu_c H).$$

Here, μ_c stands for the (giant) magnetic moment of the cluster which replaces the "μ" for single, isolated paramagnetic spins, and k is the Boltzmann constant.

In the above equation, all quantities except μ_c can be measured. The μ_c can be derived for (ideal) S.P. clusters by a curve-fitting procedure. The *gist of* obtaining the average volume $\bar{v}$ of a S.P. cluster lies in the basic physics definition of σ_s, which for a S.P. system can be written as $\sigma_s = \mu_c/\bar{v}$. There exist the low-field (LF) and high-field (HF) approximations[7, 9] of the Langevin function, from which one can calculate the $\bar{v}_{LF}$ for *large* particles (which magnetically saturate easily at low values of H/T) and $\bar{v}_{HF}$ for *small* particles (which saturate with difficulty at high values of H/T). From the $\bar{v}_{LF}$ and $\bar{v}_{HF}$, the average volume $\bar{v}$ of clusters can be estimated by taking the arithmetic mean. The LF and HF equations are stated in a later section.

It should be stressed that below a critical (Blocking) temperature (T_B) S.P. particles experience a slow relaxation time (τ) at which their net moment will align so-to-speak "parallel" to H, and thus appear to behave as if they had an apparent "bulk-like" ferromagnetic behavior. This situation will result in a hysteresis curve or an "apparent" ferromagnetic behavior. Conversely, above the T_B, the hysteresis will disappear and the particles will show a unique curve with no hysteresis.

In Mössbauer spectroscopy essentially nuclear transitions are observed between the ground and the excited states of natural isotopes, such as ^{57}Fe. These transitions are caused by γ-rays coming from a moving ^{57}Co source, which superimposes a Doppler velocity on the 14.4 keV energy and produces artificially a range of energies. Because nuclear transitions are observed, the blocking temperature T_B' observed in Mössbauer spectroscopy is quite different from the T_B found from magnetization results. In the following sections we discuss magnetization measurements, obtained for the Fe catalysts.

We have retained the classical Gaussian system of units, because these units are still used in most of the magnetics, carbon, and catalysis literature. It should suffice to point out that a field of 1 Oe = 79.6 Am^{-1} and a magnetization (σ) of 1 G = 10^{-3} Am^{-1} in S.I. units. Similarly, per gram or mass susceptibility (χ), which is often expressed as "cm^3g" or simply as "emu"/g when multiplied by 12.56 $\times$ 10^{-3} yields the S.I. (m^3/kg) units[6, 7].

The per gram saturation magnetization (σ_s, emu/g Fe) was obtained by plotting the observed σ vs $1/H$ to the lowest cryogenic temperature, and extrapolating the plots to $1/H = 0$ (i.e. at $H = \infty$). These values are recorded in Table 2 in Gaussian units. Typical plots of σ vs H for GMC and boron-doped GMC are shown in Fig. 1.

Similar plots were observed for the other samples. Plots of σ vs H/T for other samples are shown in Figs. 2–6. From these figures it is evident that a good superposition of data points from 88 to 297 K is obtained only in the case of Fe/CSX, indicating true superparamagnetic behavior over the entire temperature range for this catalyst only. For the remaining systems, a superposition of σ vs H/T occurred only above 196 K. Although measurements were made up to 473 K, for the sake of clarity the values between 297 and 88 K are presented to show the superposition; other points above 297 K also followed

Table 2. Saturation magnetization of iron (σ_s) obtained by plotting σ_{obs} vs 1/H at ~80 K

Sample	σ_s (emu/gFe)
4.8% Fe/MC	119.9
4.8% Fe/GMC	91.8
5.2% Fe/BGMC1	98.2
5.2% Fe/BGMC2	87.1
4.9% Fe/BGMC4	85.2
4.9% Fe/BGMC5	86.6
4.3% Fe/C-2	86.0
5.0% Fe/CSX	104.0

the same trend. Fe/BGMC4, Fe/BGMC5 and Fe/C-2 showed exactly similar trends in magnetic behavior to that of Fe/BGMC2 and as such are not shown here.

The working definition for a system to be superparamagnetic is that a superposition of σ vs H/T data points should occur. It follows that no hysteresis should be present in the magnetization vs H or H/T plots as the field is increased or decreased. Both these conditions are met in the supported iron catalysts reported here over a specific range of temperature. However, the observation that no superposition of data occurred from 196 to 88 K for all these carbon-supported iron systems, except Fe/CSX, suggests that these systems have a blocking temperature somewhere between 196 and 88 K. Jung and coworkers[2] also observed a similar situation with an Fe/Carbolac-1 catalyst. The importance of the blocking temperature and its relevance in assessing the region of superparamagnetism have been discussed in detail by Candela and Haines[8] and by Yamamura and Mulay[9].

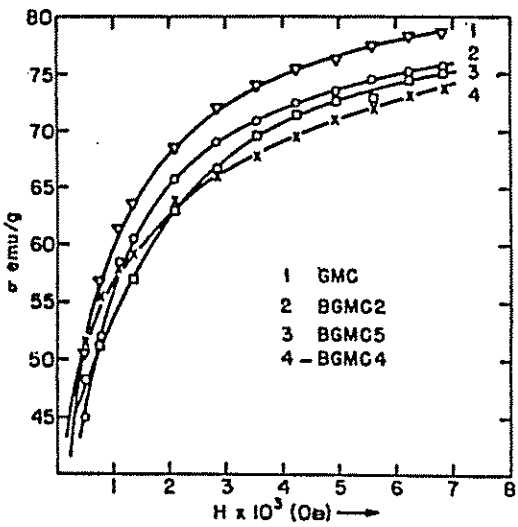

Fig. 1. Magnetization (σ) as a function of the field (H) at room temperature (296K) showing the effect of boron doping on GMC

Two important observations can be made from these magnetization measurements. First, the Fe/CSX system contains relatively small particles compared to the other systems. This conclusion has been supported by Mössbauer investigations, which are described briefly in a later section. Secondly, the Fe/(boronated carbon) systems always showed a lower magnetization as compared with the Fe/GMC system (see Fig. 3). This lowering of σ did not show any trend that could be attributed to the amount of boron added to the carbon support. This behavior is not unexpected if the boron dispersions were not homogeneous, or its concentration were too low to affect the electron density in the particles of Fe.

The observed saturation magnetizations (Table 2) were smaller than that expected for bulk Fe (217 emu/g), because of their superparamagnetic nature and the possibility of reoxidation of Fe under experimental conditions. It is interesting to note that similar values have been reported for Fe/Al_2O_3 under flowing He[10]. A particle of ferromagnetic material below a critical size consists of single domains. Such particles obviously are not confined within domain walls or boundaries and will be in a state of uniform magnetization over its entire volume. The direction of collective magnetization of an assembly of such particles behave like paramagnetic species, but with a very large magnetic moment (μ_c). Accordingly,

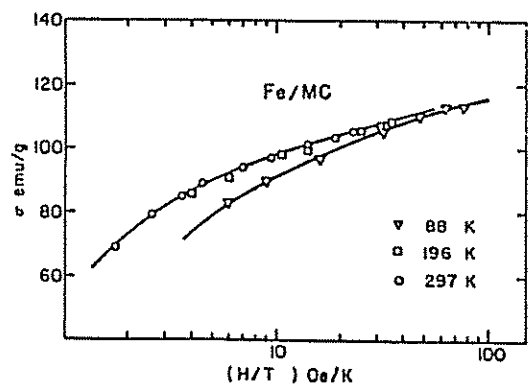

Fig. 2. Magnetization (σ) vs H/T for Fe/MC.

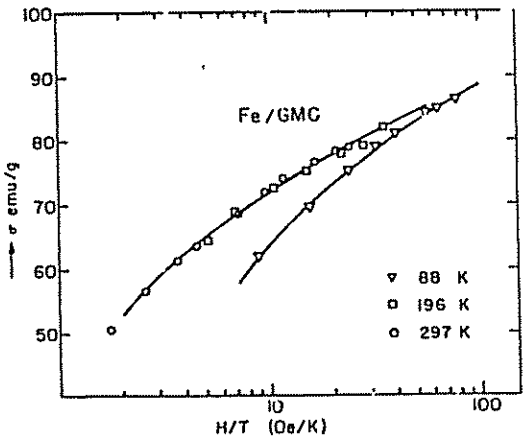

Fig. 3. Magnetization (σ) vs H/T for Fe/GMC.

the relative magnetization, σ/σ_s, of these superparamagnetic crystallites is described by the Langevin equation, which can be derived from the Brillouin function, based on quantum mechanics of spins in a magnetic field.

The working equations for computing the average particle diameter ($\bar{d}$) from the magnetization data are described in detail by Selwood[11], and are usually denoted as the Langevin lowfield (LF) and high-field (HF) approximations given by

$$\overline{d^3_{LF}} = \frac{18k}{\pi I_s}(\sigma/\sigma_s)/(H/T)$$

$$\overline{d^3_{HF}} = \frac{6k}{\pi I_s}(1 - \sigma/\sigma_s)^{-1}/(H/T),$$

where k is the Boltzmann constant, T is the measurement temperature, and I_s is the spontaneous magnetization for the bulk material. The I_s at room temperature for Fe is 1707 G[11].

It was shown in the previous section that various catalysts in the present study were found to be superparamagnetic above 196 K. Hence, using the above approach, the particle sizes in each case were estimated over the region, where the superparamagnetism was clearly evident. In the case of Fe/CSX, which showed a superposition of σ vs H/T from 88 through 297 K, the low-field and high-field particle sizes were found to be 4.2 and 3.6 nm, giving an average of 3.9 nm. For the remaining systems, the low-field and high-field particle sizes were ~ 6.0 and 5.0 nm, giving an average particle size of about 5.5 nm. The Fe particle sizes on undoped and boron-doped carbons seemed to be approximately the same.

In the literature, particle sizes have been reported in different ways. For example, some investigators simply took the cube root of the volume ($\bar{v}$), whereas some others assumed a spherical particle and reported the radius of the particle calculated from $v = (4/3)\pi r^3$. In this study calculations were based on the assumption that the superparamagnetic particles are spherical in shape and the reported values represent their average diameters ($\bar{d}$). The particle sizes deduced from the magnetization measurements ranging from 3.9 to 5.5 nm for the Fe/CSX and other systems were found to be considerably smaller than those determined by CO chemisorption studies (Table 3). This variation can be attributed to the situation that in the magnetic measurements a small amount of the sample (~0.01 g) was contained in a relatively large volume (~1 l.) of the Cahn microbalance chamber[4]. Thus, even after evacuation of the entire Faraday balance to $\sim 10^{-5}$ Pa, the reduced sample may have come in contact with O_2 from the residual gas, causing a significant oxidation of Fe° particles to γ-Fe_2O_3 and/or Fe_3O_4. This would lead to an underestimation of the size of the Fe° particles, as discussed by Jung *et al.*[2]. In contrast, this situation did not exist for the CO chemisorption measurements[2].

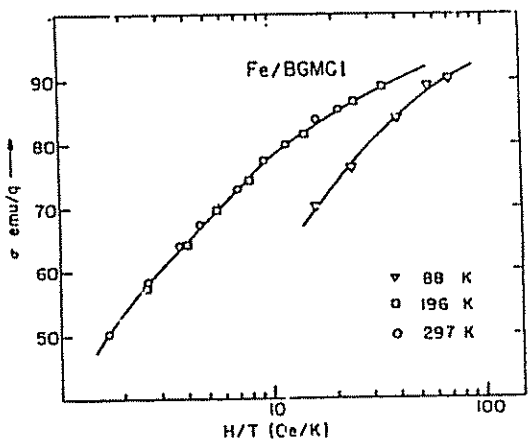

Fig. 4. Magnetization (σ) vs H/T for Fe/BGMC1.

3.2 *Mössbauer spectroscopy*

Selected supported iron catalysts were further characterized by *in situ* Mössbauer spectroscopy. Although a large number of counts were collected in the MCA, a few are shown in representative spectra for clarity. All the fresh unreduced samples, except Fe/SiO_2, gave a doublet with ΔE_Q between 0.61 to 0.76 and δ between 0.22 to 0.28 mm/sec, which are characteristic of the Fe^{3+} ion. Typical Mössbauer spectra for unreduced samples Fe/BGMC2, Fe/CSX, and Fe/SiO_2 are shown in Figs. 7(a)–(c). As presented in Fig. 7(c), unreduced Fe/SiO_2 showed a six-line pattern superimposed on a central doublet. The six-line positions corresponded to α-Fe_2O_3, whereas the central doublet corresponded to superparamagnetic particles consisting of Fe^{3+} species.

Samples of Fe/MC and Fe/BGMC1, when reduced at 673 K for 16 hr in flowing H_2 also exhibited a six-line pattern typical of ferromagnetic Fe°. On the other hand, reduced samples of Fe/Al_2O_3 (Fig. 8a), Fe/BGMC2 (Fig. 8b), and Fe/CSX (Fig. 8c) showed a central doublet along with a six-line pattern characteristic of metallic Fe°. The presence of a central doublet corresponding to the Fe^{2+} ion indicates that the iron on this support is more difficult to reduce, in agreement with previous studies[2]. In the Fe/CSX and Fe/Al_2O_3 systems, both magnetic and chemisorption studies indicated a smaller $\bar{d}$ for Fe° com-

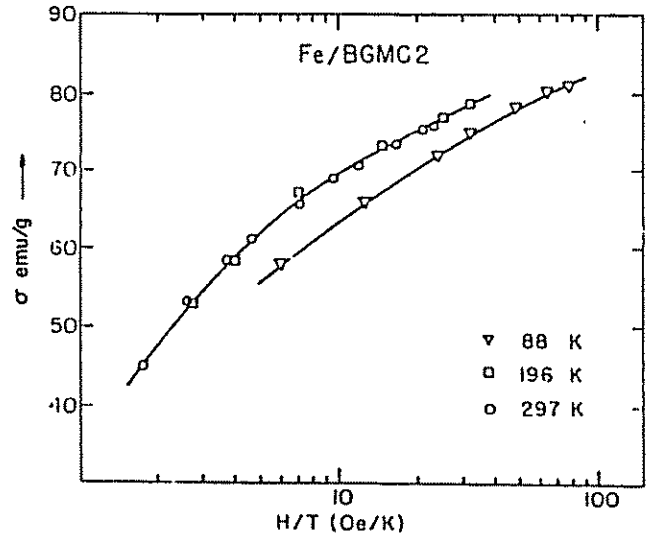

Fig. 5. Magnetization (σ) vs H/T for Fe/BGMC2.

pared to the other catalysts. For reduced samples Fe/BGMC2 (Fig. 8b) and Fe/CSX (Fig. 8c), which were found to be superparamagnetic from magnetization measurements, it was expected that a strong doublet would be obtained. However, a six-line spectrum was obtained in each case. It should be noted that a relaxation time of $\tau = 100$ sec is assumed for static magnetic measurements[11], and it is well-established that a τ in Mössbauer spectra are entirely different, because here one deals with the transitions between nuclear Zeeman levels as compared to the electronic spin orientations with respect to the applied field (H) in the static magnetic measurements. Hence, it is not surprising that in Mössbauer spectroscopy the blocking temperature T_B is much higher than 300 K in the present case. As such, sixline spectra were observed at room temperature. A discussion of these aspects is given by Boudart and coworkers[12]. In the case of reduced Fe/SiO_2, a six-line spectrum was observed; this clearly resulted from the larger particle size, as this was evident even in the fresh unreduced sample (see Fig. 7c).

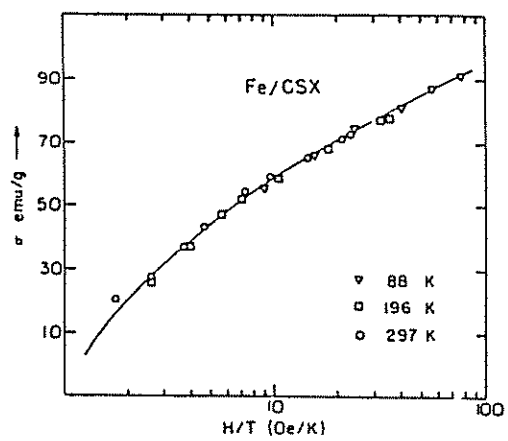

Fig. 6. Magnetization (σ) vs H/T for Fe/CSX.

3.3 *Kinetics of CO hydrogenation*

The hydrogenation of CO has been frequently used as a model reaction to study the properties of group VIII metals supported on various supports such as Al_2O_3, SiO_2, and MgO[12, 13], cage structure aluminosilicates such as ZSM-5[14, 15] and mordenites with varying Al_2O_3/SiO_2 ratios[16, 17]. However, relatively little work has been done on the use of semiconducting carbons as supports. Jung *et al.*[2] recently reported that small, superparamagnetic particles of Fe on Carbolac-1, a porous high-surface area carbon-black, are oxidation sensitive and show a somewhat decreased reducibility of Fe. These small particles (~3 nm) also showed a greatly decreased H_2/CO chemisorption ratio at temperatures up to 473 K and a high olefin/paraffin ratio, accompanied by an excellent activity maintenance, during Fischer–Tropsch synthesis. In contrast, V3G, a graphitic carbon, yielded relatively large ferromagnetic particles which gave higher specific activity comparable to other iron catalysts such as 10% Fe/Al_2O_3[2].

Recently Yoon *et al.*[3, 18] studied the benzene hydrogenation reaction over Fe supported on selected Monarch 700 carbon blacks and their graphitized forms, with and without boron doping. These catalysts were characterized by magnetic susceptibility and magnetization techniques[1]. The active catalysts had similar TOF (Turn Over Frequency) values at 448 K indicating little effect of the support on the specific activity. However, the highest achievable activities for benzene hydrogenation were obtained with the boron-doped carbon catalysts, which were 2–5 times more active than the other Fe catalysts, which included Fe/Al_2O_3 and Fe/SiO_2. The research reported in this section presents a systematic study of the effects of variation in boron doping on graphitized Monarch 700 carbon black used as supports for Fe and of the influence of this doping on the catalytic behavior of carbon-supported iron particles in the CO hydrogenation reaction.

Table 3. Activities and turnover frequencies for supported iron catalysts P = 100 kPa, T = 548 K, H_2/CO = 3

Catalyst	CO Uptake (μmole/g·cat)	Dispersion*** (Fe_s/Fe_t)	Crystallite Size (nm)	Activities (μmole/s·g-Fe) r_{CH_4}	r_{CO}	Turnover Frequency ($s^{-1}\times10^{-3}$) N_{CH_4}	N_{CO}
5.2% Fe/MC	-	-	-	26.2	64.0	-	-
4.8% Fe/GMC	27.5	0.064	12.0	20.8	56.0	18.2	48.9
5.3% Fe/BGMC1	27.0	0.057	13.0	24.5	44.0	24.7	44.0
5.2% Fe/BGMC2 (1)*	22.0	0.047	16.0	30.6	71.0	36.1	83.9
5.2% Fe/BGMC2 (2)*	22.0	0.047	16.0	29.3	78.0	34.6	92.0
4.9% Fe/BGMC4	21.5	0.051	15.0	26.1	59.0	29.8	67.2
4.9% Fe/BGMC5	27.5	0.063	12.0	29.8	77.0	26.6	68.6
5.0% Fe/CSX	60.0	0.134	5.6	2.1	4.7	0.9	2.0
5.8% Fe/SiO_2	10.5	0.020	38.0**	16.0	36.0	44.0	99.7
10% Fe/η-Al_2O_3	115.0	0.128	5.9	2.7	4.9	4.9	2.2

* (1) and (2) represent runs which were repeated with good agreement between the two.

** See text for variation in cryst. size.

*** Based on $CO_{(ad)}/Fe_s$ = 0.5

The high activities of carbon-supported iron catalysts in the present study seem to be rather unusual compared to the studies of Kikuchi *et al.*[19] or of Parkash and Chakrabartty[20]. For 1% Fe/graphite, Kikuchi *et al.* reported an activity of only 6.2 μmol CO $sec^{-1}g^{-1}$ Fe at 673 K and 100 kPa, which is much lower compared to the values obtained in the present study. However, the

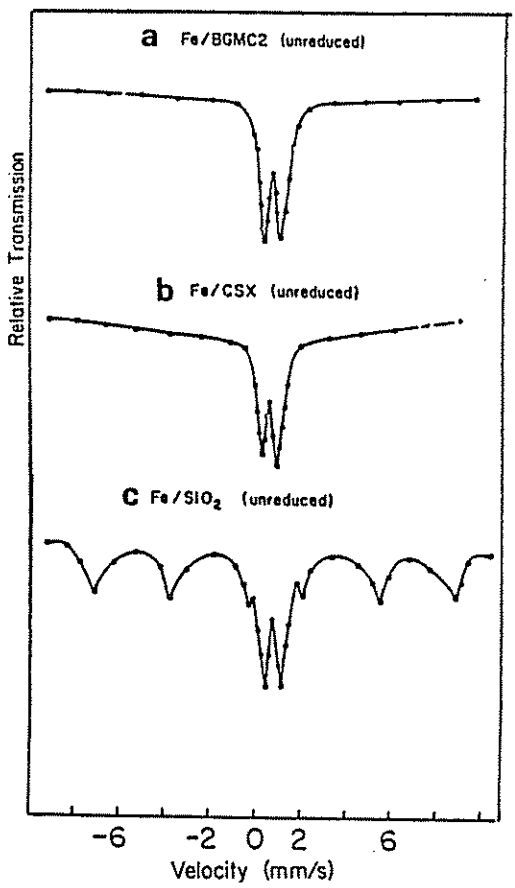

Fig. 7. Mössbauer spectra for ^{57}Fe for unreduced (a) Fe/BGMC2, (b) Fe/CSX and (c) Fe/SiO_2.

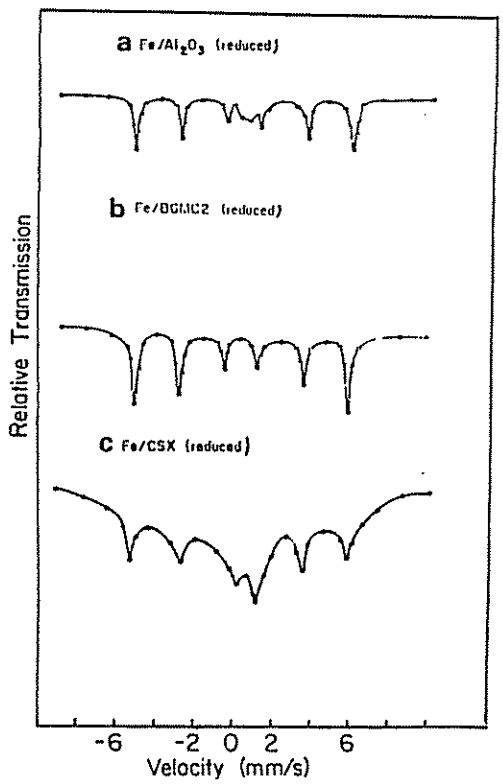

Fig. 8. Mössbauer spectra for ^{57}Fe for (a) Fe/Al_2O_3, (b) Fe/BGMC2 and (c) Fe/CSX. All reduced at 673K for 16 hr.

activities of carbon-supported Fe catalysts in this study are comparable to those reported by Jung for similar systems[2]. Storm *et al.*[21] have discussed the particle size effect in similar systems.

The turnover frequency (N) of a metal catalyst defines the catalytic activity per surface metal site and is the most characteristic parameter of the catalytic properties of the metal. The turnover frequencies given in Table 3 for methane formation and total CO conversion to hydrocarbons, N_{C_1} and N_{CO}, respectively, are calculated based on CO uptakes at 195 K to determine surface iron atoms. In these calculations, it is assumed that each adsorbed CO molecule at 195 K corresponds to two surface iron atoms in agreement with previous work[22, 23].

The following observations are noteworthy in the present study. The reaction rates, and the turnover frequencies are significantly lower for Fe/CSX as compared with Fe/MC, Fe/GMC, or Fe/boronated carbons. Secondly, boronated samples showed a small, but steady, increase in specific activity with increasing boronation, that is, with the corresponding lowering of the diamagnetic susceptibility of the support.

The lower N values of Fe/CSX are consistent with previous studies which showed that small iron particles have much lower turnover frequencies than large iron particles[2]. Both magnetization and chemisorption studies indicated a relatively smaller particle size for Fe/CSX. Thus, as observed by Jung[2] a reduction in particle size resulted in a decrease in activity. Similar observations were made in the case of Fe/MgO which showed that N_{C_1} for 5% Fe/MgO was greater by an order of magnitude than that for a similar 0.2% Fe/MgO catalyst which had a smaller particle size[12]. In the case of the Fe/Al_2O_3 catalyst used in this study, the observed activity was lower than literature values[13]; however, this is not inconsistent because of the smaller iron particle size in the present catalyst (6 nm) compared to the earlier sample (60 nm).

In the case of the boronated samples, the observed changes in N_{C_1} and N_{CO} are not large, but show a consistently increasing trend with increase in boron content. These results are presented in Fig. 9, in which the E_F of

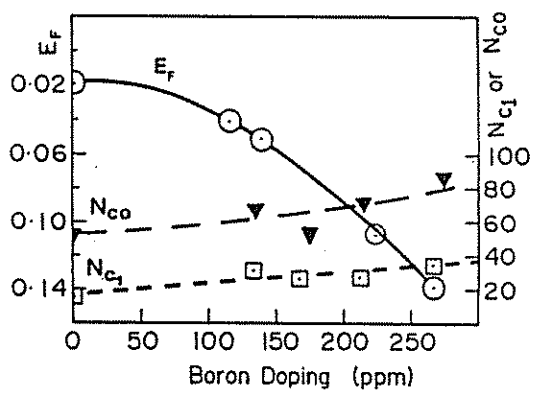

Fig. 9. The variation in the Fermi level $|E_F|$ (left hand scale using the convention in ref. 1) and the TOF for N_{CO} and N_{C_1} (right hand scale ($\times 10^{-1}$ sec ^{1}Fe, ^{1})), both as a function of boron doping.

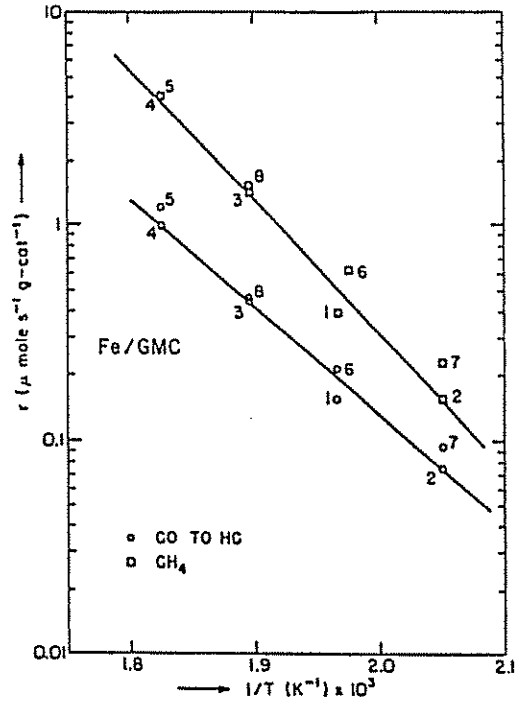

Fig. 10. Arrhenius plots for the conversion of CO to HC and CH_4 observed for Fe/GMC.

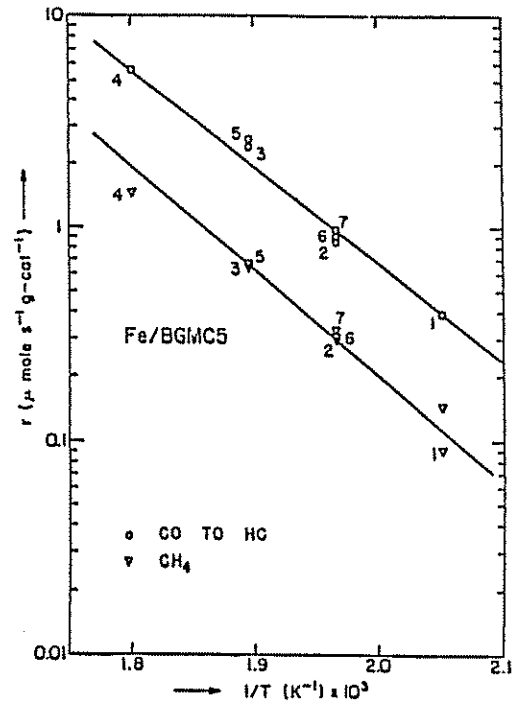

Fig. 11. Arrhenius plots for the conversion of CO to HC and CH_4 for Fe/BGMC5.

Table 4. Activation energies for CO hydrogenation over supported iron catalysts

Catalyst	E_{C_1} (kJ·mole^{-1})	E_{CO} (kJ·mole^{-1})
5.2% Fe/HC	93.1	107.7
4.8% Fe/GHC	95.6	114.6
5.3% Fe/BGHC1	91.0	101.0
5.2% Fe/BGHC2	103.1	119.6
4.9% Fe/BGHC4	97.2	115.1
4.9% Fe/BGHC5	95.5	101.5
4.3% Fe/C-2	86.3	97.1
5.0% Fe/CSX	103.0	118.0
5.8% Fe/SiO_2	96.3	107.3
10% Fe/η-Al_2O_3	80.0	84.8

the carbon supports, N_{C_1}, and N_{CO} are plotted against the B content. The observed changes in N_{C_1} and N_{CO} lie outside the range of experimental error, and these values double as the B content increases to 260 ppm so that they are nearer to N_{CH_4} and N_{CO} values for Fe/SiO_2 and for large Al_2O_3-supported Fe crystallites[2, 3].

Arrhenius plots were drawn from the reaction rates measured at different temperatures for CO hydrogenation over supported iron catalysts, and apparent activation energies were computed from such plots for both methanation and total conversion of CO to hydrocarbons, denoted by E_{C_1} and E_{CO}, respectively. Typical Arrhenius plots are shown in Figs. 10 and 11. The activation energies were computed using a least-squares fit and the corresponding values are shown in Table 4. The data points are numbered to denote the chronological order of the kinetic runs. Good agreement is observed for measurements in ascending and descending sequences of kinetic runs, which indicates that a stable iron surface could be maintained for each kinetic run by using the bracketing technique to minimize deactivation processes. The activation energies for methanation and total CO conversion are similar over all the carbon-supported iron catalysts and are in good agreement with values reported earlier[3]. These results showed no clear-cut trend with changes in support characteristics, again in agreement with previous work by Jung *et al.*[2].

Product distributions for the various supported iron catalysts were found to be consistent in both ascending and descending sequences of kinetic runs between 488 and 548 K. These distributions of C_1 to C_5 hydrocarbons formed at 528 and 548 K along with the CO conversion and the ratio of olefins to paraffins ($C_2 - C_4$) are given in Tables 5 and 6. Low molecular weight paraffins are clearly the predominant products, as expected for large, unpromoted iron crystallites[18]. The presence of boron in the carbon has no discernible effect and clearly does not enhance olefin formation.

As stated before, Fig. 9 shows the variation in E_F of carbon supports and the TOF for CH_4 and CO conversion, both as a function of the boron doping. It is evident from this figure that as the E_F is lowered by boron doping[11], a small increase is observed in N_{C_1} and N_{CO}. This allows the possibility that there may be a small support effect

Table 5. Product distribution for various Fe catalysts at 528 K

Catalyst	% CO Conv. to HC	Product Distribution (mole %)							Olefin/Paraffin Ratio
		C_1	$C_2^=$	C_2	$C_3^=$	C_3	C_4	C_5	
5.2% Fe/HC	1.55	69	2	7	4	7	6	4	0.43
4.8% Fe/GHC	1.10	70	3	14	-	4	5	3	0.18
5.3% Fe/BGHC1	2.20	76	-	16	-	7	8	-	-
5.2% Fe/BGHC2	1.76	70	2	7	5	5	5	4	0.58
4.9% Fe/BGHC4	1.46	67	3	15	3	5	5	2.5	0.30
4.9% Fe/BGHC5	1.75	64	3	14	4	5	5	3	0.35
4.3% Fe/C-2	1.57	64	5	14	2	2	5	4	0.44
5.0% Fe/CSX *	0.85	74	-	22	-	-	3	2	-
5.8% Fe/SiO_2	1.34	68	1	19	-	7	3	2	0.04
10% Fe/η-Al_2O_3 *	2.35	73	-	24	-	14	7	1	-

* Reaction temperature = 523 K

Table 6. Product distribution for various Fe catalysts at 548 K

Catalyst	% CO Conv. to HC	Product Distribution (mole %)							Olefin/Paraffin Ratio
		C_1	$C_2^=$	C_2	$C_3^=$	C_3	$C_4^=$	C_5	
5.2% Fe/MC	3.36	67	2	15	4	4	5	3	0.32
4.8% Fe/GMC	2.50	65	1	18	-	7	4	2	0.04
5.3% Fe/BGMC1	3.90	76	3	17	-	2	1	1	0.16
5.2% Fe/BGMC2	3.71	68	1	15	2	5	4	2	0.15
4.9% Fe/BGMC4	2.92	68	2	17	2	5	4	1	0.18
4.9% Fe/BGMC5	3.78	63	3	18	4	6	5	1	0.29
4.3% Fe/C-2	3.69	64	5	14	7	2	4	2	0.75
5.0% Fe/CSX *	3.10	61	3	27	-	7	1	1	0.09
5.8% Fe/SiO_2	2.10	68	1	19	-	7	3	2	0.04
10% Fe/η-Al_2O_3 *	5.39	69	-	21	-	5	5	1	-

*Reaction temperature = 543 K

in these carbon-supported iron catalysts; however, the nature of this effect, should it be verified, is not obvious as there are several possible explanations. These include a Fe-particle size effect[2, 21] and the possibility that the Fe particles may be in contact with boron on the surface of carbon supports.

4. SUMMARY

Supported iron catalysts were prepared by impregnating various undoped and boron-doped carbons with an aqueous $Fe(NO_3)_3$ solution. These catalysts were characterized by *in situ* magnetization measurements as a function of the field and temperature. From plots of σ vs H/T, which showed superparamagnetic behavior, average particle sizes of metallic iron were estimated using the Langevin low-field and high-field approximations[9]. These particle sizes ranged from 3.8 to 5.5 nm. Iron dispersed on carbons boronated up to 260 ppm, in general, exhibited lower saturation magnetization than Fe dispersions on undoped carbon. However, no obvious trend was evident in the magnetization values which could be attributed to either an inhomogeneous distribution of the boron atoms in the carbon network or to boron concentrations too low ($\leq$260 ppm) to significantly alter the electron density of supported iron particles.

The supported iron catalysts were further characterized by Mössbauer spectroscopy. The fresh unreduced catalysts gave a central doublet indicative of a superparamagnetic α-Fe_2O_3. Fe/carbon (CSX), when reduced at 673 K, indicated a significant fraction of superparamagnetic particles, in agreement with the magnetic and chemisorption studies. The other systems, when reduced, gave a six-line spectrum, which is attributed to a blocking temperature, which was higher than the measurement temperature.

Although the E_t of the carbon supports decreases substantially by B doping, only a small increase in the turnover frequency for methane and for CO conversion occurred. A number of explanations can account for this behavior, such as a small support effect either by a direct interaction between iron and the carbon support or by modification of active sites at the iron–carbon interface, modification of iron particle morphology, direct promotion of B–Fe contact, or an Fe particle size effect. A choice among these cannot be made at this time.

Hydrogenation of CO was performed over these catalysts and from the reaction rates at different temperatures, parameters such as activation energies, product distributions and turnover frequencies were obtained. For Fe/carbon (CSX) the catalytic activity was somewhat lower over the catalysts with the smallest Fe crystallites, in agreement with previous studies. In general the electronic properties of carbons had little or no effect on the catalytic and magnetic properties of Fe.

Acknowledgements—We are grateful to the National Science Foundation, USA, for supporting this work with an NSF Grant No. CPE 7915761. One of us (Prasad Rao) is thankful to the Government of India for providing him with a fellowship during 1979–83.

REFERENCES

1. L. N. Mulay, A. V. Prasad Rao, P. L. Walker, Jr., K. J. Yoon and M. A. Vannice, Doped carbon black catalyst supports: I. Characterization by magnetic susceptibility and ESR spectroscopy. *Carbon* **23**, 493 (1985).
2. H.-J. Jung, M. A. Vannice, L. N. Mulay, R. M. Stanfield and W. N. Delgass, *J. Catal.* **76**, 208 (1982); see also H.-J. Jung, P. L. Walker, Jr. and M. A. Vannice, *J. Catal.* **75**, 416 (1982); and H.-J. Jung, Ph.D. Thesis, The Pennsylvania State University (1981).
3. K. J. Yoon, P. L. Walker, Jr., L. N. Mulay and M. A. Vannice, *Ind. Engrg. Chem. Prod. Res. Dev.* **22**, 519 (1983).
4. L. N. Mulay, *Magnetic Susceptibility*, A Reprint Monograph. Wiley, New York (1966); and Krieger Publishers, Melbourne, FL (1980). See also Chapter in *Physical Methods of Chemistry*, (Edited by A. Weissberger and B. W. Rositter), Vol. I, Part IV. Wiley, New York (1972).
5. W. N. Delgass, L. Chen and G. Vogel, *Rev. Scient. Instrum.* **47**, 968 (1976).
6. L. N. Mulay and I. L. Mulay, *Anal. Chem.* **50**, 274R (1980); **52**, 199R (1982); **54**, 293R (1984).
7. L. N. Mulay and E. A. Boudreaux, (Eds.), *Theory and Applications of Molecular Diamagnetism* and *Theory and Applications of Molecular Paramagnetism*, Wiley, New York (1966).

8. G. A. Candela and R. A. Haines, *Appl. Phys. Lett.* **34**, 868 (1975).
9. H. Yamamura and L. N. Mulay, *J. Appl. Phys.* **50**, 7795 (1979).
10. V. Perrichon, P. Turlier, J. Barrault, J. O. Forquy and J. C. Menezo, *J. Appl. Catal.* **1**, 169 (1981).
11. P. W. Selwood, Chemisorption and Magnetization. Academic Press, New York (1975).
12. M. Boudart, J. A. Dumesic and H. Topsøe, *Proc. Natl. Acad. Sci. USA* **74**, 806 (1977).
13. M. A. Vannice, *J. Catal.* **37**, 449 (1975); **37**, 462 (1975); **44**, 152 (1976).
14. C. Lo, K. R. P. M. Rao, L. N. Mulay, V. U. S. Rao, R. T. Obermyer and R. J. Gormley, in *Mössbauer Spectroscopy and Its Chemical Applications* (Edited by J. G. Stevens and G. K. Shenoy). Advances in Chemistry Series 194, Am. Chem. Soc., Washington (1981).
15. R. T. Obermeyer, C. Lo, M. Oskooie-Tabrizi V. U. S. Rao and L. N. Mulay, *J. Appl. Phys.* **53**, 2683 (1982).
16. M. Oskooie-Tabrizi, C. Lo and L. N. Mulay, *Proc. Intermag. Conf.* Philadelphia, April 1983, *IEEE Mag. Trans.* **19**, 2001 (1981).
17. T. Pannapariyal, C. Lo, M. Oskooie-Tabrizi and L. N. Mulay, *J. Appl. Phys.* **56**, 2601 (1984).
18. K. J. Yoon and M. A. Vannice, *J. Catal.* **82**, 457 (1983).
19. E. Kikuchi, T. Ino and Y. Morita, *Bull. Jap. Petro. Inst.* **18**, 139 (1976).
20. S. Parkash and S. K. Chakrabartty, *Carbon* **15**, 307 (1977).
21. D. Storm and M. Boudart, 6th N. Am. Catal. Soc. Meeting, Chicago, March (1979).
22. M. Boudart, A. Delbouille, J. A. Dumesic, S. Khammouma and H. Topsøe, *J. Catal.* **37**, 486 (1975).
23. P. H. Emmett and S. Brunauer, *J. Am. Chem. Soc.* **59**, 319 (1937).